

This is an Open Access document downloaded from ORCA, Cardiff University's institutional repository:<https://orca.cardiff.ac.uk/id/eprint/137760/>

This is the author's version of a work that was submitted to / accepted for publication.

Citation for final published version:

Gomaa, Mohamed, Jabi, Wassim , Veliz Reyes, Alejandro and Soebarto, Veronica 2021. 3D printing system for earth-based construction: case study of cob. Automation in Construction 124 , 103577. 10.1016/j.autcon.2021.103577

Publishers page: <http://dx.doi.org/10.1016/j.autcon.2021.103577>

Please note:

Changes made as a result of publishing processes such as copy-editing, formatting and page numbers may not be reflected in this version. For the definitive version of this publication, please refer to the published source. You are advised to consult the publisher's version if you wish to cite this paper.

This version is being made available in accordance with publisher policies. See <http://orca.cf.ac.uk/policies.html> for usage policies. Copyright and moral rights for publications made available in ORCA are retained by the copyright holders.



3D Printing System for Earth-based construction: Case Study of Cob

Mohamed Gomaa^{a*}, Wassim Jabi^b, Alejandro Veliz Reyes^c and Veronica Soebarto^a

^a School of Architecture and Built environment, Horace Lamb Building, University of Adelaide, Adelaide SA5005, Australia.

^b Welsh School of Architecture, Bute building, Cardiff University, Cardiff, CF10 3NB, United Kingdom.

^c School of Art, Design and Architecture, Roland Levinsky Building, University of Plymouth, PL4 8AA, United Kingdom.

*Corresponding Author: mohamed.gomaa@adelaide.edu.au ;

Postal address: School of Architecture and Built environment, Horace Lamb Building, University of Adelaide, Adelaide SA5005, Australia

Phone: (+61) 0413088466

Abstract

Despite the dramatic development in digital manufacturing technologies in the recent years, 3D printing of earth materials, such as cob, still presents several challenges to the market-available 3D printing systems. This paper describes the development process of a 3D printing system for cob that fits the contemporary requirements of digital construction. The study first described the methodology of producing a revised cob recipe for the purpose of 3D printing. Then, the study conducted thorough investigations into the properties of three types of extrusion systems using both electromechanical and pneumatic methods, leading eventually to the development of a new bespoke dual-ram extruder. The study then explored systematically the relationship between the new 3DP system and the rheological properties of cob, followed by an exploration to the new geometric opportunities the new system offers. The study findings show that the new extrusion system improves greatly the 3DP process of cob in terms of extrusion rate, continuity, consistency, and mobility. The findings are expected to bring 3D printed cob construction closer to full-scale applications. On a broader scale the study contributes to the disciplines of architectural design and construction by providing a framework capable of bridging the knowledge gap between vernacular modes of building production and contemporary digital practice.

Keywords

3D printing; Additive manufacturing; Robotic construction; Digital fabrication; Extrusion systems; Cob; Earth-based material.

33

1. Introduction

34 An increasing amount of research on implementing 3D printing (3DP) systems for large-scale
35 formats has exposed multiple potential applications for architecture and the construction
36 industry (Tay et al. 2017; Wu, Wang, and Wang 2016). Concurrent research highlights the
37 advantages of 3D printing in construction to achieve a higher degree of process optimisations
38 (e.g. financial, construction time, staffing resource), the emergence of new digital processes
39 associated to Building Information Modelling and potential for mass customisation, and
40 environmental benefits towards the life cycle of 3D printed objects and building elements (Wu,
41 Wang, and Wang 2016). Additionally, research such as the review paper by Tay et al. (2017)
42 outlines environmental benefits of 3DP in construction as a result of a reduced use of formwork
43 (Kothman and Faber 2016).

44 Cob stands as one of many types of earth construction methods and it had been utilised
45 historically all over the world. Its mix consists of subsoil (earth), water, and fibrous material
46 (typically straw). However, similarly to related construction methods, cob buildings embody a
47 material mix, as well as its associated construction method. Cob walls are typically built using
48 hand-made material deposition on top a plinth, then corrected (e.g. correction of vertical
49 planes) with material added or removed before or after drying (Hamard et al. 2016). As a result,
50 building elements can comprise a variety of geometries, yet the builder is required to constantly
51 negotiate the execution of an intended design with ever-changing material properties (e.g.
52 water content, drying speed) necessary to achieve the design goals without the need for
53 formwork or any mechanical compaction method (Figure 1). As a result:

- 54 • Cob provides a high degree of design freedom and adaptability throughout the
55 construction process, where the builder negotiates with the material (and its properties)
56 as the building process proceeds (Veliz Reyes et al. 2019), challenging the normalised
57 view of robotic 3D printing as a linear process from design to production.
- 58 • Cob can be reutilised throughout the construction process, providing the opportunity
59 for testing and prototyping design solutions (Kennedy, Smith, and Wanek 2015),
60 reducing the amount of waste material and enabling low-cost project corrections and
61 modifications on-site.
- 62 • Recent research demonstrates that cob complies with modern regulations such as UK
63 building performance standards (Goodhew and Griffiths 2005).
- 64 • When compared to other massing construction materials and methods (e.g. concrete),
65 cob has lower CO₂ emissions, low embodied energy (Benardos, Athanasiadis, and
66 Katsoulakos 2014) and requires a lower degree of depletion of natural resources
67 (Goodhew and Griffiths 2005).

68 These criteria suggest that a 3D printing system of cob warrants further investigation as a
69 potential pathway toward more sustainable 3DP practices, with a lesser environmental impact
70 when compared to concrete 3D printing (Alhumayani et al. 2020). Recent evidence supports
71 this observation; an early study conducted on small material samples (Gomaa et al. 2019)
72 provides evidence that 3D printed cob elements have competitive thermal performance
73 standards when compared to other materials such as concrete, brickwork, and conventional cob
74 construction.

75



Figure 1. Exposed cob construction in Totnes, UK.

76

77

78

79 Hamard et al. (2016) and Agustí-Juan et al. (2017b) highlight that the integration of digital
80 fabrication techniques with vernacular modes of architectural production can reveal
81 sustainability potentials for construction applications as compared to other cement-based 3D
82 printing methods. This, mainly due to existing forms of cob knowledge production (e.g.
83 vernacular construction techniques), emerges from long-lasting local environmental, material,
84 social and skills contexts of construction practice. This research recognises the potential of
85 developing building technologies associated with vernacular knowledge and building practices,
86 generating a research and development process highly grounded on responsible innovation by
87 leveraging local industries and technologies, utilising local materials and workforce (Garrett
88 2014). Moreover, the study challenges normalised models of design-to-fabrication research by
89 incorporating local, vernacular and material knowledge as a methodological consideration and
90 engagement process throughout the study. This negotiation between disparate frameworks of
91 material practice (detailed in Veliz Reyes et al, 2019), established both in R&D research and
92 in vernacular construction, not only results in emergent material opportunities within a standard
93 design-engineering professional delivery framework but also enables novel methodological
94 approaches to architectural tectonics, local materials and skillsets, digital discourses and
95 building technologies.

96 A substantial share of recent research on 3DP for construction addresses 3D printing of cement
97 and mortar-like materials. As a result, there has been a huge development in 3D printing
98 systems for cement-based materials in recent years (Geneidy, Ismaeel, and Abbas 2019; Shakor
99 et al. 2019). Different types of extrusion systems are currently used for 3D printing; varying
100 from pneumatic pumps and electromechanical ram extruders. In spite of these developments,
101 3D printing of earth-based materials, such as cob, still presents several challenges to the
102 market-available 3D printing systems such as material granularity, material properties and mix
103 ratios, or the use of local organic fibres, which must addressed through extensive experimental
104 research before delivering a feasible construction method (Veliz Reyes et al. 2018). These
105 requirements highlight the opportunities of vernacular knowledge as a source of digital
106 innovation, as it has already tested, iterated and perfected mix ratios and earthen architecture
107 production typologies around the world.

108 Following early studies of cob 3DP technology (e.g. Veliz Reyes et al, 2018) the sensitivity of
109 the printing process to the material mix is currently a major limiting factor in the development

110 of construction-scale 3D printing with cob. The hardening property of the material mix creates
111 a critical constraint on the speed of the 3D printing process (Perrot, Rangeard, and Courteille
112 2018; T. T. Le et al. 2012). The interrelation between hardening time and printing velocity
113 must be monitored carefully, as each printed layer must be hard enough to support the weight
114 of the successive layers. At the same time, the material mix must sustain a certain rheological
115 behaviour that enables it to be extruded smoothly through the 3DP printing system (Perrot,
116 Rangeard, and Pierre 2016; Veliz Reyes et al. 2018), despite its irregular granularity and
117 addition of organic material. Moreover, effective design of material delivery systems may
118 offset some irregularities that may be unavoidable in a commercial application, particularly
119 considering the effect of specific geological, environmental or geographic conditions on the
120 quality of 3DP cob mix.

121 Panda and Tan (2018) demonstrated the importance of establishing a clear understanding of
122 the rheological behaviour of highly viscous 3D printed materials such as concrete. One of the
123 major issues with 3D printing of such materials is to balance between the fluidity level and
124 sufficient viscosity simultaneously in a way to ensure smooth flow of material through the
125 extrusion system without clogging while maintaining the extruded material shape during the
126 printing process. In concrete 3D printing, the developed mixtures must be thixotropic in nature,
127 which means it should have high yield stress and low viscosity (Panda, Unluer, and Tan 2018).
128 Other studies by Lipscomb and Denn (1984), (Le et al. (2015) and Choi, Kim, and Kim (2014)
129 also highlighted the critical influence of mixture components, such as particle size, gradation,
130 surface area and paste/aggregate volume on the flow property of the material as they govern
131 the yield stress and viscosity. In his study, Perrot et al. (2016) proposed a theoretical framework
132 for the structural built-up of 3DP of cement-based materials. His proposal showed the
133 correlation between vertical stress acting on the first deposited layer with the critical stress
134 related to plastic deformation that is linked to the material yield stress.

135 In earth construction, the rheology of the material is the key to control the quality of the
136 structures. Historically, adjusting the consistency of cob mixtures depended greatly on the on
137 the local know-how, simply though controlling the water to soil ratios, or by adding other
138 ingredients such as fibres or lime (Perrot, Rangeard, and Lecompte 2018). As the construction
139 industry shows a growing interest in earth materials via 3D printing, the need to develop simple
140 and rapid testing for estimating earth material workability and rheological properties has
141 increased (Bruno et al. 2017; Khelifi et al. 2013). According to Perrot, Rangeard, and Lecompte
142 (2018), field-oriented tests can be leveraged to estimate material parameters such as the yield
143 stress, which will provide important information to describe the rheological behaviour of the
144 earth material. Weismann and Bryce (2006) demonstrated in their book “Building with cob: a
145 step-by-step guide” detailed the methods for simple field tests of subsoil and cob
146 characteristics. The recommended testing procedures were established on historical methods
147 for building with cob, all aiming to provide clear understanding of the subsoil workability and
148 rheology properties.

149 This research leverages the qualities of cob construction to utilise it as a groundwork for digital
150 innovation through robotic 3D printing of building elements. This line of research has
151 maintained the craft quality of cob as a source of innovative knowledge, often developed
152 outside the boundaries of professional and academic frameworks - a “vernacular”
153 understanding of the material usually communicated through making and practice instead of
154 standard academic communication pathways (Niroumand, Barceló Álvarez, and Saaly 2016).

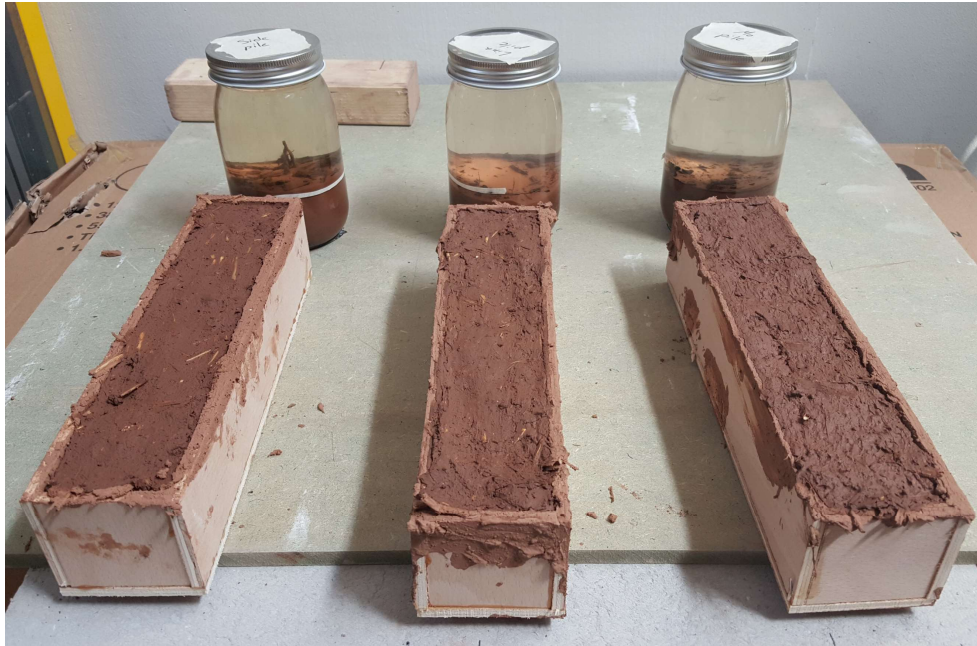
155 This evolutionary approach of vernacular architecture as a driver for novel environmental,
156 technological and cultural discourses is exploited in this study through an iterative design
157 research method, which has developed a material mix for cob 3D printing applications, an
158 innovative extrusion system for cob 3D printing applications, and a series of tests attempting
159 to outline emerging large-scale design opportunities resulting from this technology.

160 **2. Methods and Material**

161 **2.1. Material**

162 In cob construction, printing material properties must be considered and formulated carefully
163 according to both its wet and hardened states. Wet properties are those related to the material
164 in its fresh, or ‘green’ state, i.e. the state that the material is in from initial mixing to the point
165 at which it is deployed on site, before drying or hardening (Perrot et al. 2018a). According to
166 Le et al., (2012), three basic criteria must be met to ensure a successful 3D printing process;
167 extrudability, buildability, and workability with time. This means that the material must flow
168 efficiently through the system without excessive force and be deposited in layers with minimal
169 deformations. At the same time it must be able to support the loads of subsequent layers before
170 hardening and reaching some degree of structural integrity. The transition from printing to
171 hardening must occur within a time frame considering the material hardening rate while
172 meeting the overall construction requirements such as tolerances for deformation. A similar
173 process is conducted during hand constructed cob, as the builder must skillfully negotiate water
174 contents, structural integrity and building design throughout the construction process.

175 In the context of this study, mix ratios have been reached through an iterative process of testing
176 and material characterisation. Weismann and Bryce (2006) and Hamard et al. (2016)
177 recommended that the composition of a cob mixture (averages) to be 78% subsoil, 20% water
178 and 2% fibre (straw) by weight. The recommendation for the subsoil formula itself is 15-25 %
179 clay to 75-85 % aggregate/sand. This mix, however, requires adaptation for 3D printing
180 applications that maximises its fluidity, while maintaining printability properties (e.g. layer
181 definition) and structural cohesion (e.g. layer height). This study used subsoil sourced from a
182 farmland near Cardiff, UK, for the cob specimens. Subsoil specimens were examined according
183 to the recommended testing methods in the literature (Steve Goodhew, Grindley, and Probeif
184 1995; Weismann and Bryce 2006): shake test, brick test, sausage test, ball drop test. These tests
185 utilized simple deposition tests in order to acknowledge typically utilized on-site tests as well
186 as to eventually simplify the material characterization process should this method be used in
187 different contexts with little or no access to material testing facilities (Figure 2).



188

189 *Figure 2. Shake and brick tests to the three subsoil samples from Cardiff.*

190 However, as cob is traditionally mixed in a nearly dry state, the recommended compositions
191 above do not necessarily fit the purpose of 3DP applications where a less viscous rheology is
192 required. Lower water content in the mix leads to higher friction between the material and
193 extrusion cycle parts, creating massive pressure on the extrusion mechanisms, resulting in
194 increasing wear rate of the parts and reduce the long-term efficiency and printing quality.
195 Gomaa et al. (2019) conducted a number of systematic tests to reach suitably modified
196 proportions of cob mixtures for 3D printing purposes. The testing process included systematic
197 alteration of several factors. Water contents of 22, 24, 26, and 28% were tested. The study
198 concluded that the water content in the 3D printed cob mixture should be increased to an
199 average of 25% while straw remains at 2%, resulting in a subsoil percentage of 73% (by
200 weight).

201 It was anticipated that the increase in the water content will alter the rheology of the cob mix
202 during and after the extrusion process. Therefore, it was important to examine the behaviour of
203 the cob mix under the extrusion force. This examination seeks a systematic understanding of
204 the variation in the printed path size in relation to the extrusion rate through the nozzle and
205 motion speed on one side, and nozzle size and layer height on the other. Extrusion rate is
206 usually used to express the volume of material passing through a given cross sectional nozzle
207 area per unit time (mm^3/sec). Linear extrusion rate, on the other hand, represents the passing
208 length of the material over unit time (mm/sec) (Khan Academy 2015; Zareiyan and Khoshnevis
209 2017). The study at first examined the synchronization process between linear extrusion rate
210 and motion speed. Linear extrusion is chosen so that changes in the cross sections of different
211 nozzles will not alter the outcome. Yet, the study focused on understanding the vital relation
212 between the layer height and nozzle size, and their impact on the printed outcome.
213 Understanding this relation is essential during the process of transforming the designed
214 geometry into accurate contours and path lines for the 3D printing framework. The correct, and
215 accurate, estimation of the 3D printed size of path lines and the geometry in total increases the
216 quality of the outcome.

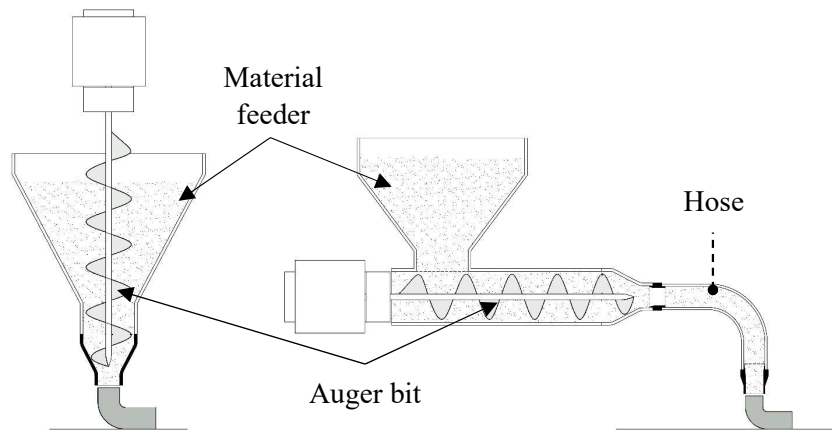
217 A series of tests were conducted to define this relationship mathematically. The tests set the
218 nozzle diameter and the motion speed as constants at 45 mm and 80 mm/sec respectively, with
219 a synchronised linear extrusion rate at 105 % of the nozzle motion speed (approximately 85
220 mm/sec). The printed file consisted of five path lines. Each line had a different layer height,
221 starting from 15 mm and ending at 35 mm with 5 mm intervals. Each printed line was then
222 measured and assigned to its respective height. This test was repeated three times to observe
223 any possible variation to the outcome and increase credibility of estimations.

224 **2.2. Equipment**

225 A complete 3D Printing (3DP) system consists of two separate devices: a motion controller
226 and a material delivery system. The two must be designed in coordination to realise the final
227 3D printed outcome: the weight of the extrusion system can affect the motion controller, or the
228 accuracy of the motion controller can affect the tolerance and deformation of the final printed
229 element. The study used a 6-axes KUKA KR60 HA robotic arm as the motion controller. The
230 computer software package for robotic control was Rhinoceros via Grasshopper and KUKA
231 PRC®. The material delivery system is the part of the printer setup which stores, transports,
232 and deposits the print medium. The design of the material delivery system is vital to successful
233 printing, as the material must be layered with enough accuracy, at a consistent and
234 synchronized extrusion rate with the robot motion. Not meeting these needs can easily
235 jeopardise the resulting print quality, which could significantly affect the shape and the
236 structural integrity of a printed element. The material delivery tool (i.e. the extrusion system)
237 replicated commercial clay extruders that exist in the market, which usually use both pneumatic
238 and electromechanical techniques. The study then developed a new bespoke extrusion system
239 which will be detailed later in the paper.

240 **2.3. Extrusion system**

241 Two types of material extrusion methods were tested in this research; 1) Screw-pump, and 2)
242 Ram extrusion. The screw pump is a method that utilises an auger screw in order to transport
243 and compress the material to a specific point, which in the case of 3D printing is the nozzle.
244 Upon rotation, the screw acts as a type of rotational positive displacement pump, transporting
245 material in the axial direction of the screw (Figure 3). Auger extrusion systems may be
246 vertically or horizontally oriented. The screw sits within a material hopper, which is filled with
247 material to be extruded. The rotating screw then pulls the material through the system. This
248 method is used by the WASP Company in their Delta 3MT and 12MT printers, which they
249 used to experiment with 3D printing of earth-based materials (Figure 4) (3D-WASP 2020).



250

251 *Figure 3. Two types of the screw pump: vertical screw (left) and horizontal screw (right)*

252



253

254

Figure 4. Screw pump extruder by WASP

255 In ram extruders, a linear force is applied on a piston inside a cylinder ram filled with the
 256 material. The generated pressure then forces the material through the nozzle once a threshold
 257 of pressure is reached. These systems are also commercially known as linear actuators. The
 258 exerted force in linear actuators is generated by two methods (Figure 5);

259 1) Pneumatic, using air/gas, by increasing the pressure on one side of a pneumatic cylinder,
 260 leading to linear motion and an applied force on the plunger of the extrusion device.

261 2) Electromechanical, using lead screw or screw-jack, which translates circular motion from a
 262 motor into the linear motion and force exertion required to extrude the material.

263

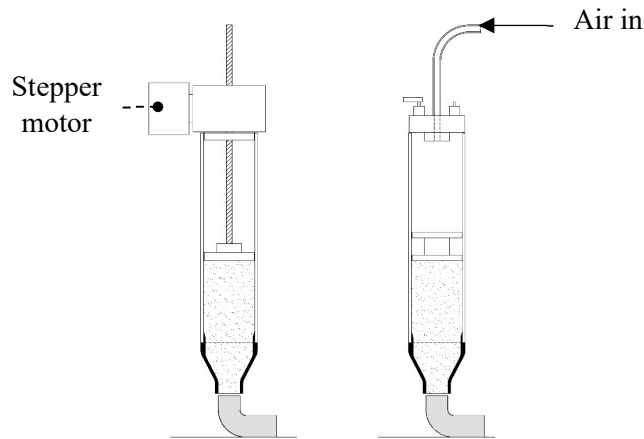


Figure 5. Scheme of the Pneumatic (right) and electromechanical (left) ram extruders.

2.4. Prototyping and Geometry

The prototyping process included two stages; the first stage is the calibration of the 3D printing settings, and the second stage is geometry prototyping. The calibration of settings is an important step to enhance the relationship between the robotic arm and the extrusion system. The calibration process was designed as a set of 3D printed path lines with variable layer heights and speeds. An understanding of the material behaviour is pursued through observing the relationship between the layer height, extrusion rate and nozzle dimension. The applied changes in the layer heights varied from 15 to 35 mm. These heights are chosen to represent a range of ratios in relation to the nozzle size, which has a diameter of 45 mm.

The second stage of prototyping focused on the geometry potentials and limitations. The main aim of this step is to examine several geometrical challenges that encounter the robotically assisted 3D printing of cob such as the inclined surfaces, arch based shapes and maximum height per printing period. The maximum height per printing period reflects the achieved geometry height before pausing the printing process until the printed geometry gain structural strength through the transformation process from wet to dry state (3D WASP 2016). Additionally, it must be acknowledged that cob can be reutilised after printing, either through the modification of a printed object (while still wet) or through trimming excess cob from already set built elements. As a result, the geometric and prototyping processes of cob 3D printing comprise an iterative quality which facilitates testing.

3. Results and Discussion

3.1. Extrusion System

3.1.1. Bespoke Screw pump

Inspired by the vertical screw extrusion system in the commercial Delta12MT WASP® (Figure 4), the research team developed a screw pump based on an auger bit device. The initial concept was to create a more robot-friendly extruder, where the material feed point was stationary and the extruded material was delivered to the robot arm end-effector point through a hose. This design concept aimed to provide a higher freedom of movement for the robot, besides an

295 improved practicality of material feeding technique as compared to the available cob and clay
296 extrusion system in the market, which requires regular human interference with the extruder
297 for material feeding while on the move.

298 The used device for this testing was a repurposed auger conveyor, originally designed to
299 transport sand. Alterations were made in order to make it suitable for cob extrusion (Figure 6).
300 The initial testing of the device showed remarkable improvement in terms of extrusion rate,
301 consistency and scale of the printed outcome. It was able to achieve a maximum extrusion rate
302 of 80 mm/sec with a 50mm nozzle diameter. However, this system revealed several major
303 shortcomings that required further stage of developments:

- 304 • The extruder jammed consistently due to the build-up of straw and rough aggregate at
305 two points in the system; one at the interface between the auger tip and the nozzle and
306 another at the interface between the hopper (feed point) and the auger.
- 307 • It still required constant human interaction to feed the material through the hopper.
- 308 • The whole mechanism was heavy and relatively large, which compromised the freedom
309 of movement of the robot, and consequently limiting the complexity level of the
310 geometry designs.
- 311 • The attempt of making the screw device stationary and install a hose at the screw end
312 (as shown in Figure 3- right) was unsuccessful. Installation of the hose increased both
313 the load and the material travel distance beyond the auger direct contact surface. The
314 increase in hose length has an inverse proportional relation with the extrusion rate,
315 accompanied by noticeable material retraction at the feeding point.

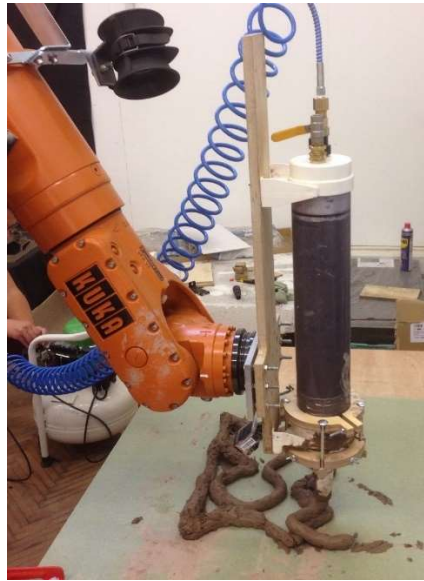


316
317 *Figure 6. The prototype of the bespoke screw pump.*

318 3.1.2. Pneumatic

319 The experimentation of this extrusion type was inspired by most of the industrial clay and
320 concrete extruders, which are based on exerting linear force by using pneumatic pumps. The
321 study used a pneumatic linear ram extruder, in which the pressure was manually controlled.
322 The ram cylinder had a maximum capacity of 4000 ml and the used nozzle size was 30 mm
323 Figure 7. The system was compact enough to be mounted easily on the robot arm and enable
324 remote control of system at the same time. Despite the acquired strength from this extruder,
325 the use of pneumatic system for a dense material like cob revealed a series of challenges in
326 terms of controlling the extrusion rate, quality and consistency of extrusion. Furthermore, it

327 required consistent human interaction throughout the print process to adjust the extrusion rate,
328 fix faults and prevent collapses.



329

330

Figure 7. The pneumatic linear ram extruder

331 3.1.3. Electromechanical

332 In order to overcome the drawbacks of the pneumatic system, the study switched again to the
333 use of the electromechanical extrusion method in its third phase. This phase used a commercial
334 small size screw-jack extruder provided by 3D potter ® (Figure 8). The benefit of a screw-jack
335 is that it includes a gearbox, providing extra torque at a lower speed. The new system provided
336 a better control over the extrusion rate and consistency due to the use of a stepper electric
337 motor, which resulted in a higher print quality. However, this extruder by 3D potter is designed
338 to execute small-medium size prototypes of clay-based materials, as the standard maximum
339 nozzle size was 16 mm. The system had to be modified by attaching a larger 25mm bespoke
340 nozzle to be more suitable for cob extrusion. Despite the dramatic increase in the printing
341 quality, the new system suffered from a slow printing speed limited to 5 mm/sec due to the
342 increased nozzle size. This rate of 3D printing had restricted the progress of the
343 experimentation, while it also restricted the scale of the printed outcome which may represent
344 actual wall in a building. Furthermore, the capacity of the material container was too small
345 (3000ml) for a large print to be made without refilling, and the process of refilling the device
346 was slow as it required almost a partial disassembly of the whole extruder (Veliz Reyes et al.
347 2018).



Figure 8. The electromechanical linear ram extruder and its 3D printed outcome.

348

349

3.1.4. Bespoke electromechanical dual ram extruder

351 All the previous experimentations of different extrusion methods have led to the development
 352 of a completely new extrusion method that can accelerate the creation of prototypes, leading to
 353 an increased productivity and greater research potentials. The previous three experimentations
 354 have exposed five critical challenges that face robotically assisted 3D printing of cob:

- 355 1) Continuity of printing process.
- 356 2) Maximum extrusion rate.
- 357 3) Consistency and quality of outcome.
- 358 4) The freedom of movement.
- 359 5) Reduction of human interaction (remote control).

360 Each tested extrusion system exhibited a number of advantages and limitations. Table 1
 361 summarises the efficiency level of each tested extrusion system based on the five previous
 362 criteria. The efficiency levels are expressed as Low, Medium and High, where low refers to
 363 limitations and high refers to advantages.

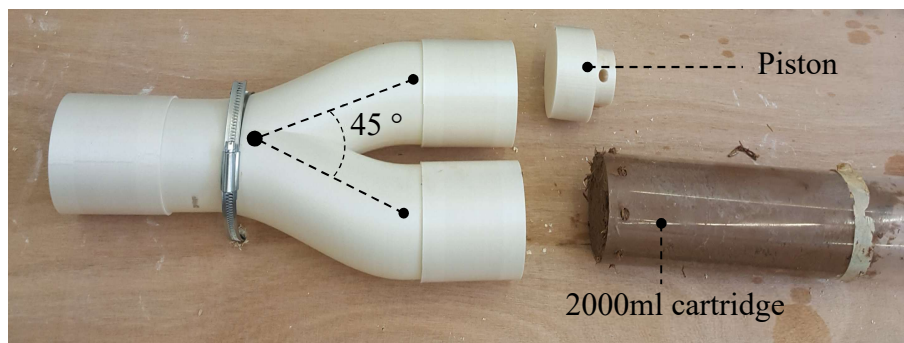
Table 1. Efficiency level of the tested criterions of each extrusion systems

	Continuity	Extrusion rate	Consistency	Movement Freedom	Human interaction
Screw pump	Medium	High	Medium	Low	Low
Pneumatic	Low	Medium	Low	Medium	Medium
Electromechanical	Low	Low	High	Medium	Medium

364 These criteria are crucial challenges to improve the workability and productivity of 3D printed
 365 cob research and practice. The successful encounter of these issues will open the window for
 366 more sophisticated explorations on both the 3DP cob mix properties and the geometry design
 367 aspects. Out of all the previous three introduced extruding systems, the electromechanical
 368 linear ram has shown promising potentials in overcoming the five challenges. However, it
 369 suffered mainly from the slow extrusion speed and the lengthy process of material reloading.
 370 Therefore, it has become important to build a new -off the shelf- extrusion system, inspired by

371 the core concept of electromechanical screw jacks and capable of tackling the limitations of
372 the previous systems.

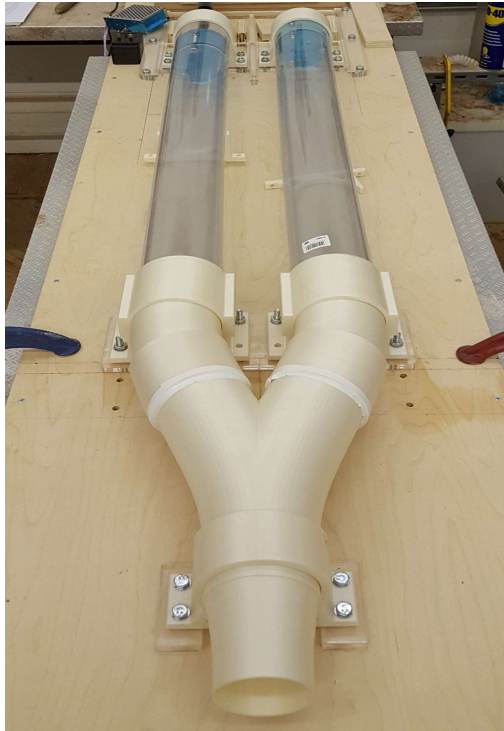
373 The design process of the new system went through different iterations of trials and failures
374 before reaching the final design. The initial concept started with the aim of building a simple
375 upscaled version of the existing electromechanical screw jacks, shifting it from a single 2000ml
376 cartridge to a single 8000ml, while adding a quick release system to accelerate the refill
377 process. However, while this partially solved the issue of material quantity, it did not solve the
378 continuity issue as the system still required to be on hold while the cartridges were being
379 replaced. To solve this problem, an auxiliary cartridge was added in order to cover the hold
380 time for the main cartridge to be replaced, but with the two cartridges working sequentially.
381 The concept was inspired by small scale PLA and ceramic dual extruder by Leu et al. (2011)
382 and 3D-WASP (2020). The first trials were proofs of concept, where preliminary prototypes of
383 the system were made in 1:4 scale using 3D printed plastic parts. These trials used the standard
384 2000ml cartridges from the existing 3D potter electromechanical screw jack (Figure 9). The
385 dual joint tested two different angles (45° and 22.5°) to ensure a smooth merge of the material
386 between the two channels. The lower angle (22.5°) showed a smoother merge, hence it was
387 selected to be applied in the full-scale prototype.



388

389 *Figure 9. Initial proof of concept of the system in 1:4 scale using the 45 degrees dual joint.*

390 The full-scale prototype initially used 3D printed plastic joints and fixtures. The whole system
391 was then fixed on a mobile plywood platform (Figure 10). The first set of tests of the prototype
392 showed success in terms of proving the workability of dual extrusion concept, yet it revealed
393 two critical flaws which affected the extrusion process. The plastic parts were receiving a huge
394 amount of pressure externally from the screw jacks and internally from the material flow, which
395 eventually led to a quick wear and destruction of the parts at the mounting points (Figure 11-
396 left). In addition, the accumulating pressure along the axis between the screw jack mounting
397 point and the dual joint mounting point made the plywood platform buckle from the middle.
398 This buckling forced the cartridge to bend, leading to a material leakage then eventually a
399 massive crack in the plastic cartridge (Figure 11-right and Figure 12). Therefore, to avoid these
400 flows in the final prototype, it was obvious that the system components must be fabricated from
401 stronger materials such as aluminium, whereas the platform must be reinforced with a metal
402 structure to prevent bending. The extrusion system can then be mobile by mounting the whole
403 platform on a mobile table.



404

405 *Figure 10. The initial full-scale prototype using 3DP PLA joints and fixtures on a plywood platform.*



406

407 *Figure 11. Destruction of the 3DP PLA joints due to pressures caused by the cob mix (left) and the*
 408 *destruction of the cartridge due to pressures caused by the bending plywood platform (right).*



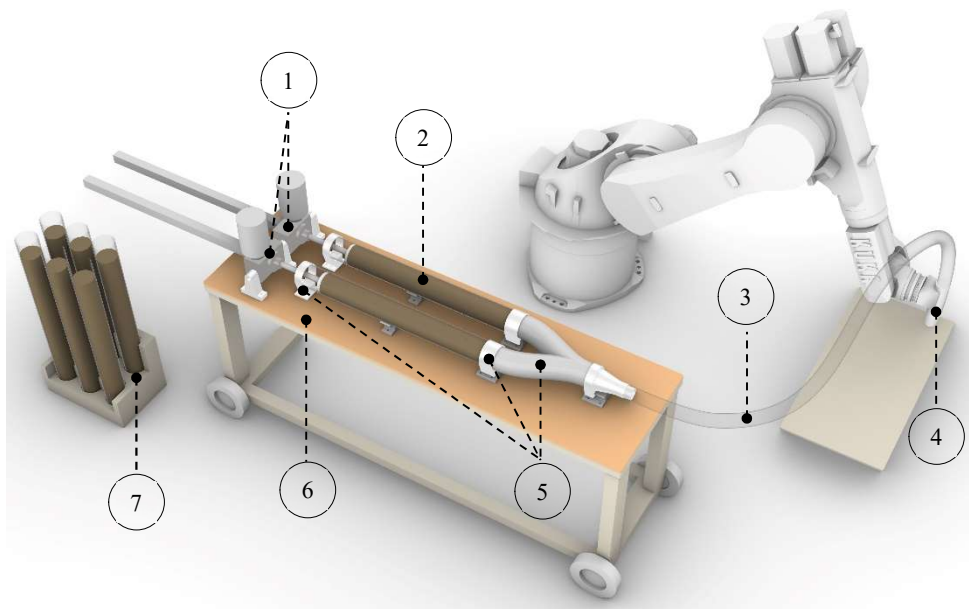
409

410 *Figure 12. Buckling of the plywood platform due to accumulated pressures on mutnig points*

411 The final system prototype introduces a bespoke extrusion system with a unique dual-cartridge
 412 design (Figure 13, Figure 14). Each cartridge has a capacity of 8000 ml (total of 16000ml both)
 413 and powered by a heavy-duty electric screw jack. The screw jacks are supplied by ZIMM®

414 with 25 kN nominal capacity, leveraging a 1000 mm stroke and capable of delivering 80
415 mm/sec operating travel speed. The screw jacks are powered by two 3-phase motors, 0.75kW
416 each. The motors combine electromagnetic braking system that ensures immediate stop to the
417 stroke, which minimizes the dynamic response. These specs were specially requested based on
418 calculations of the expected loads in the system, considering factors such as the material weight
419 inside the system and the desired extrusion rate. As budget was limited, some adjustment to
420 the system design were applied to simplify the manufactured parts and reduce the cost without
421 affecting the targeted efficiency. Figure 13 shows a scheme of the bespoke dual extruder
422 different components.

423 Material cartridges and screw jacks are connected together by bespoke aluminium parts, which
424 are designed to provide smooth and fast reloading process. The most distinctive aluminium
425 part is the Y-shaped joint that merges the material dual flow from both cartridges into a single
426 flow then feed it to a hose. The used hose is 3-meter-long, made from PVC with a steel-wire
427 reinforcement. The complete system is mounted on a mobile platform, allowing transitions
428 around the robotic arm.

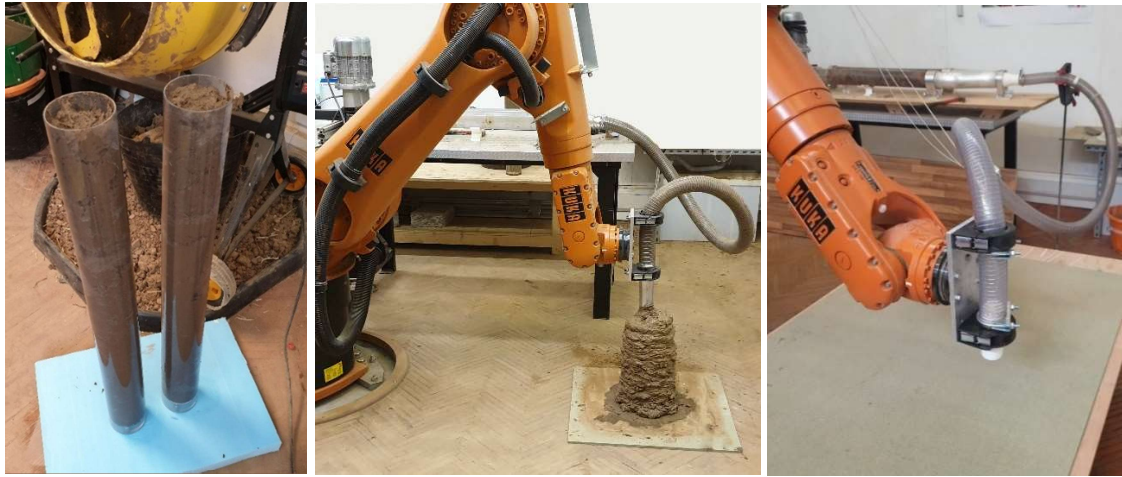


429

430 *Figure 13. Scheme of the new bespoke dual extruder components: 1) Screw jack, 2) Cob Cartridge, 3)*
431 *Steel-wired PVC hose, 4) Nozzle, 5) Aluminum parts, 6) Mobile platform, 7) Cartridges Rack.*



432



433

434 *Figure 14. The components of the bespoke dual extruder.*

435 The new system was tested extensively through sequence of calibrations and prototyping
 436 process, which took place as part of an experiential studio on 3D printing of cob at the Welsh
 437 School of Architecture in Cardiff University. The system proved to be successful in
 438 overcoming the five previous challenges as follows:

439 1- Continuity of printing process:

440 The new system adopts a sequential process of extrusion based on dual lines of cartridges. This
 441 process can be described in 6 steps as shown in Figure 15:

442 Step 1: The process preparation starts by loading two filled cob cartridges on the platform.
 443 Each cartridge, with its attached screw jack, form a line of extrusion. Few other cartridges are
 444 filled with the required amount of cob for the whole print and kept in a rack, ready to be loaded
 445 on the system later.

446 Step 2: The printing process starts by pumping cob through one cartridge at a time using one
 447 screw jack (line 1), simultaneously with initiating the robotic arm motion to exert the required
 448 design.

449 Step3: As the operating screw jack on line 1 reaches its stroke end, it stops and immediately
 450 triggers the second screw jack to start pumping cob through the second cartridge on line 2 while
 451 the first screw jack is retracting. After the complete retraction of the first screw jack, the empty
 452 cartridge is removed and a full cartridge is reloaded.

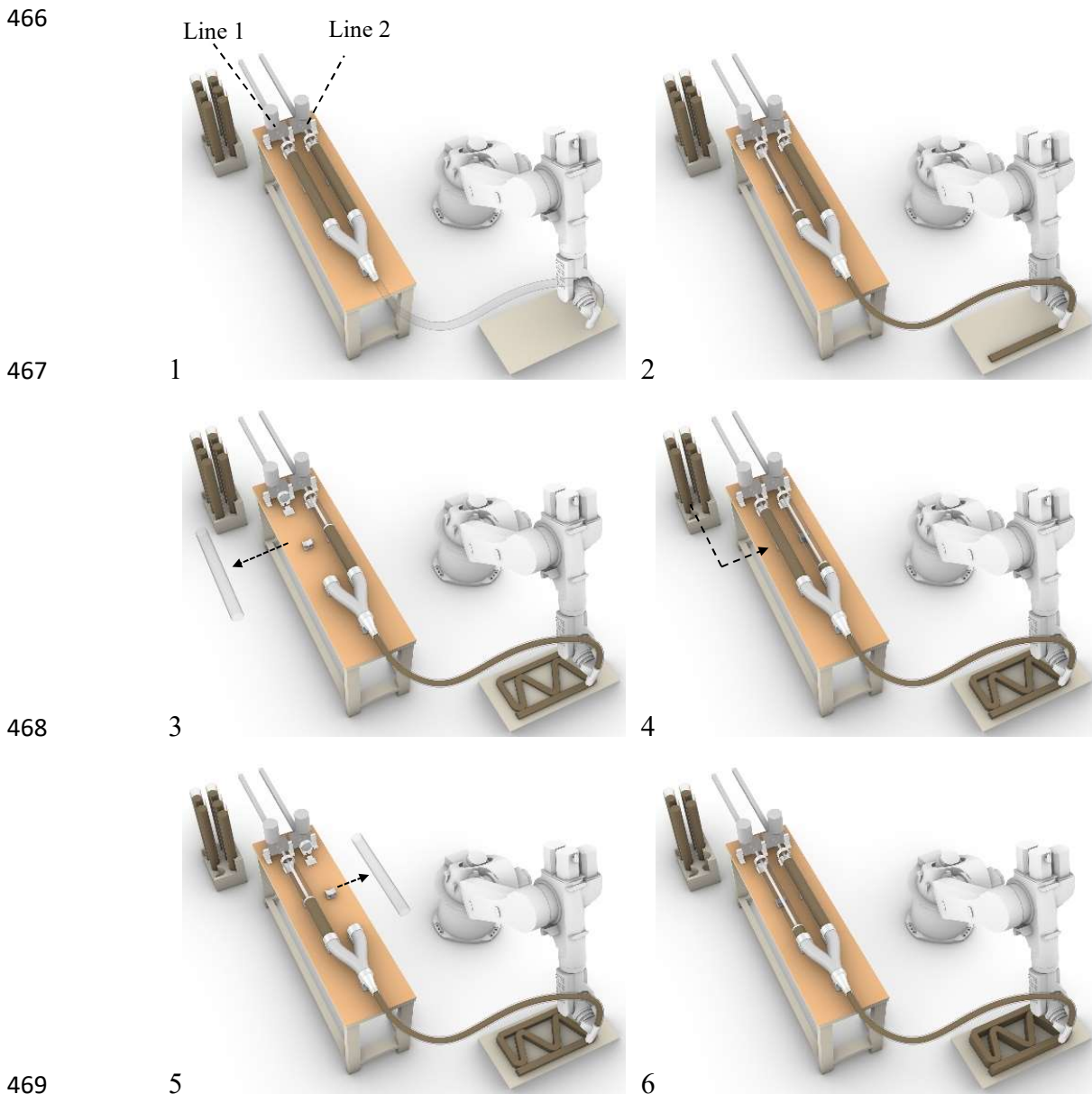
453 Step 4: By the time the first cartridge is reloaded, the operating cartridge will be reaching its
 454 end of stroke, which then releases the stopping brakes and triggers the first screw jack to start
 455 pumping cob through the first cartridge while the second screw jack is retracting.

456 Step 5: After the complete retraction of the second screw jack, the empty cartridge is removed
 457 and a full cartridge is reloaded on line 2.

458 Step 6: The process then repeats sequentially until the end of the required 3D printed outcome.

459 It is recommended to estimate the whole required amount of material before the printing
 460 process, then preparing either the exact number of cartridges (for small tasks) or just a few
 461 extra cartridges and store them in a rack. This will create a buffer margin between the process
 462 of refilling and reloading, which will ensure continuity of the process and constant flow of cob
 463 throughout the whole process, with no need to interfere, stop or slow it down. The special

464 design of the aluminium parts also enhances the continuity of the process as they combine rails
465 with latching mechanism, offering smooth reloading of cartridges on the platform.



470 *Figure 15. The six steps of the extrusion process in the bespoke dual extruder.*

471

472 2- Maximum extrusion rate:

473 The upgraded screw jacks can deliver up to 80mm/sec operating travel speed. Using
474 this travel speed with a 45mm diameter nozzle elevates the extrusion rate of cob on the
475 nozzle to 120mm/sec, which is nearly 20 times faster than the previous small linear ram
476 extruder with 30 mm nozzle. However, based on calibration tests, it was found that 50
477 to 80mm/sec extrusion rate is sufficient for most of the geometry testing in this project.
478 Moderate speeds offer a relaxed reloading process and gives time to extruded layer of
479 cob to strengthen slightly before receiving the subsequent layers.

480 3- Consistency and quality of outcome:

481 The new screw jack by ZIMM leverages a 25KN ball screw gearbox and 3-phase motor
482 controlled by variant frequency driver (VFD). This enables a steady operational torque and an
483 accurate control over travel speed, which provides a consistent flow of cob. This consistent
484 flow dramatically improves the quality of the printed outcome as compared to the previous
485 extruders.

486 4- Freedom of movement

487 The new system uses a hose to link between the main body of the extruder on the platform and
488 the nozzle point. This minimises the mounted mass/ load on the robot's end-effector, as now it
489 only carries the nozzle joint with the hose instead of carrying the whole extruder as in the
490 previous pneumatic and small electromechanical linear ram extruders. Minimising the contact
491 size between extruder and robot enables more degrees of freedom for the robot to move,
492 resulting on broader complexity levels in the geometry design if needed. Moreover, the
493 platform itself is mobile and can be easily moved around the robot if required to compensate
494 the possible limitation in the hose length.

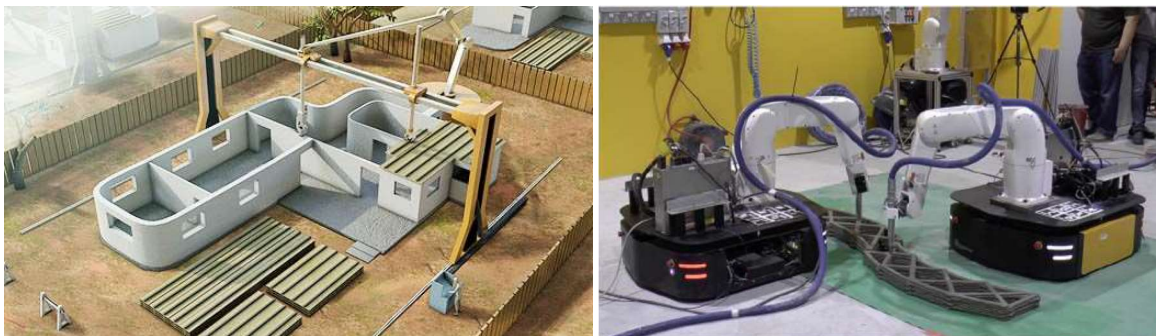
495 5- Reduction of human interaction (remote control)

496 The new system is designed to separate between the material feeding point on the platform and
497 the extrusion point on the robot's end-effector. This separation enables the reloading of the
498 cartridges without the need to interrupt (stopping or slowing down) the robot movement. The
499 cartridges system and the simple latching mechanism of aluminium parts also minimise the
500 time required for reloading and reduce human interaction time consequently.

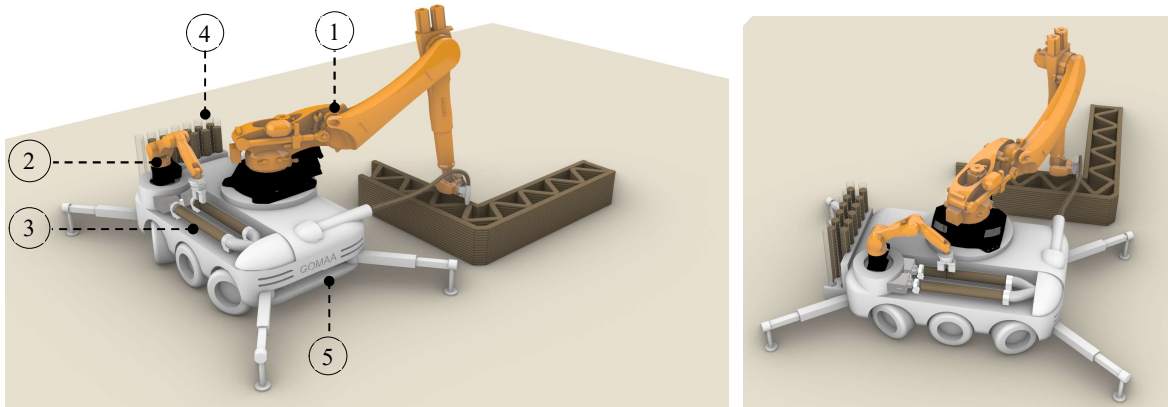
501 3.1.5. Remarks on the dual extrusion system

502 Besides the five previous advantages, the simple, yet innovative, design of the new extrusion
503 system made it replicable and also affordable to build as compared to the available commercial
504 options. Moreover, the design enables the system to operate either as a single or dual extruder
505 with different nozzle sizes. This facilitates the 3D printing process for small and medium size
506 prototypes without the need to operate the full system. In addition, the new system has potential
507 for successful implementation into full autonomous large-scale 3D printing process. The study
508 suggests leveraging two on-site 3D printing concepts for that purpose; first one is inspired by
509 mobile crane 3DP system by Contour Crafting (2020) Figure 16-left, where the robotic arm
510 and the extrusion system can be combined in the crane system. The second is inspired by the
511 mobile robotic vehicles which is presented in a study by Zhang et al. (2018) Figure 16- right.
512 A revised design for mobile robot vehicle that can combine both the extruder and the
513 collaborative robotic station is suggested as in Figure 17.

514



515 *Figure 16. Mobile crane system for 3DP by Contour crafting (left), mobile robotic vehicles by Zhang*
 516 *et al (2018) (Right)*



517
 518 *Figure 17. Design of mobile robot vehicle combining both the cob extruder and the collaborative*
 519 *robotic station. 1)Primary robot for printing. 2) Secondary robot for cartridges reloading. 3) Cob*
 520 *extruder. 4) Cartridges rack. 5) Autonomous robotic vehicle.*

521 It is however important to state that the system is an initial prototype that also requires some
 522 enhancements and future upgrades. The current design still depends on human interaction to
 523 initiate and terminate the 3D printing process, in addition to preparing the cob mixtures,
 524 refilling and reloading the cartridges on the platform. It also very important to follow good
 525 practice while filling the cartridges to avoid air pockets and inconsistency, which causes high
 526 dynamic response. Also, the current material capacity is limited to 12.0 kg/cartridge, which
 527 forces large number of refills to print a real scale wall. For example, 1×1×0.5 m cob wall would
 528 require nearly 45 cartridges. Another current limitation is associated with the hose length.
 529 Increasing the hose length over 3 meters was found to be harder to mount on the robot and
 530 creates higher resistance towards moving and bending. Longer hose is also harder to be cleaned
 531 from cob leftovers after each printing process. Therefore, several planned upgrades will
 532 involve:

- 533 • Connecting the VFDs (controllers) of the screw jacks directly to the Robot controller
 534 unit, where the extruder will be operated simultaneously with the robot using the same
 535 code file.
- 536 • Increasing the material capacity of the system through upgrading the screw jack power
 537 and the cartridges volume. Moreover, the current dual-piston design could be redesigned
 538 to combine four pistons, capable of accommodating four cartridges at a time.
- 539 • The introduction of a collaborative robotic process, where a smaller robot arm will be
 540 part of the extruder platform to execute the cartridge reloading task. The required amount
 541 of material will be calculated ahead of the process, then translated into a number of
 542 cartridges. Another machine will be dedicated for mixing and refilling the empty
 543 cartridges while the prefilled cartridges are being used in the extruder.
- 544 • Implementing a shutter mechanism over the main dual AI connections can add extra
 545 layer of controllability as it will prevent any possible backflow of material during the
 546 cartridge reloading process. The current system design, however, does not suffer from
 547 material backflow due to the acute angle (45 degrees) of the dual AI piece and the
 548 relatively high viscous nature of the cob mix.

549

3.2. Material mix properties

550 The increased water content to 25 % in the new 3DP cob composite, instead of 20% for
 551 conventional cob composite, has shown satisfactory extrusion in terms of consistency and
 552 quality of extrusion. It was naturally anticipated that the increase in fluidity has proportional
 553 relation to the rheology of the cob mix during and after the extrusion process. First set of tests
 554 explored the synchronization process between extrusion rate and robot motion speed. It was
 555 clear from the start that the extrusion rate must be synchronised with the motion speed of the
 556 robotic arm on a 1:1 rate at least. Slower rate of extrusion will result in an intermittent printed
 557 outcome as can be seen in Figure 18-left. On the contrary, increasing the extrusion rate in
 558 relation to the robot motion speed (using a constant layer height) will result in a more consistent
 559 print and wider path lines. In Figure 18-right, the path lines A and B reflect a ratio of 1.15:1,
 560 while path lines C and D reflect a ratio of 1.05:1. The increased ratio of extrusion rate to motion
 561 speed results in wider path lines under a constant layer height. Table 2 below describe the
 562 relationship between extrusion rate and robot arm motion speed.



563

564 *Figure 18. Explorations of the synchronization process between extrusion rate and robot motion*
 565 *speed (left & right)*

Table 2. Relationship between extrusion rate and robot arm motion speed

Path line code	A-B	C-D	Unit
Nozzle diameter (D)	45	45	mm
Layer height (h)	15	15	mm
Extrusion rate	92	85	mm/sec
Robot motion speed	80	80	mm/sec
Path width (w)	88	70	mm
Extrusion rate to motion speed ratio	115	105	%

566

567 The study concluded after several trials that 3D printing with a liner extrusion rate of 105-
 568 110% of the robot motion speed (1.1:1) considered favourable due to the nature of the cob mix,
 569 where there are chances of having inconsistent sections of materials inside the cartridges that
 570 cause slight interruptions in the extrusion rate from time to time. It is possible to overcome this
 571 issue by installing an extrusion rate sensor at the nozzle end that can give live feedback to the
 572 variant frequency driver (VFD) of the actuator to make the proper adjustments to power. Worth
 573 mentioning that the study also observed that the slightly higher extrusion rate has a “ramming

574 effect” on the printed outcome, where the printed path lines becomes denser and gain more
 575 structural strength with each new printed layer.

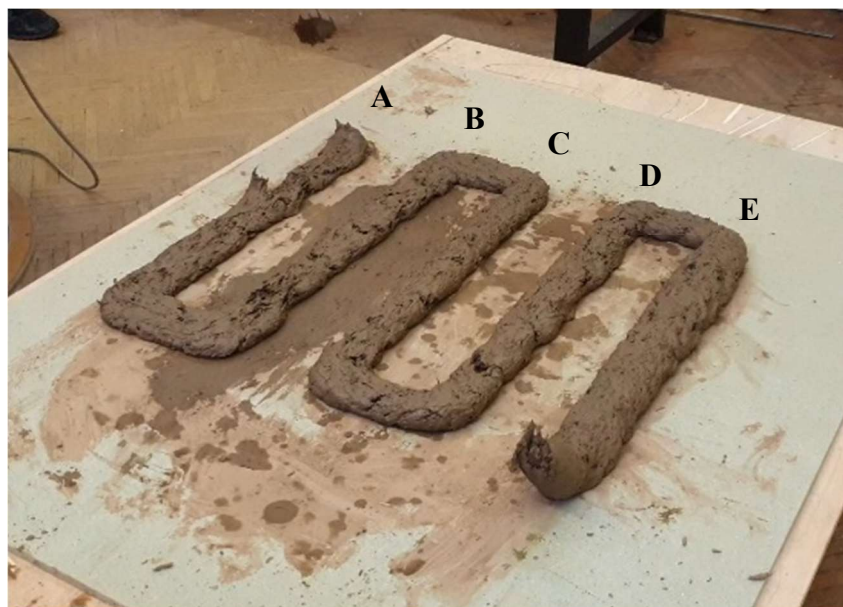
576 The second set of tests on the relationship between the layer height, nozzle size and path line
 577 width has improved the understanding of their influence on the 3D printed outcome and
 578 printing process in general. As can be seen in Figure 19, each printed path line (A to E) is
 579 designed to reflect the relation between a specific layer height and its respective path width,
 580 where the extrusion rate to robot motion speed ratio is set to 110% as advised previously, and
 581 the nozzle size is fixed at 45mm. The layer heights started with 15 mm at path line A, then the
 582 heights were increased discretely with 5 mm increment per each path line, ending with 35 mm
 583 layer height at path line E. Each increase in the layer height exhibited a decrease in the path
 584 line width. These relationships between the change in layer heights and path line width has
 585 been recorded and described as the expansion factor in Table 3. This test eventually resulted in
 586 a model that can estimate the path line width in accordance to the layer height and the nozzle
 587 size (Figure 20).

588 The linear relationship presented in Figure 20 can be described using the following equation:

589
$$\text{Estimated path line width (mm)} = \text{Nozzle size (mm)} \times \text{Expansion factor}$$

590 where the expansion factor can be obtained from the chart. To explain further; for example;
 591 under a synchronised motion speed and linear extrusion rate, with a 45mm in diameter
 592 extrusion nozzle and 25mm layer height (layer height is 56 % of the nozzle size) and an
 593 expansion factor of 1.6, :


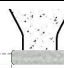
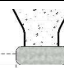
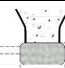

594
$$\text{Estimated path line width (mm)} = 45 \times 1.6 = 70 \text{ mm}$$



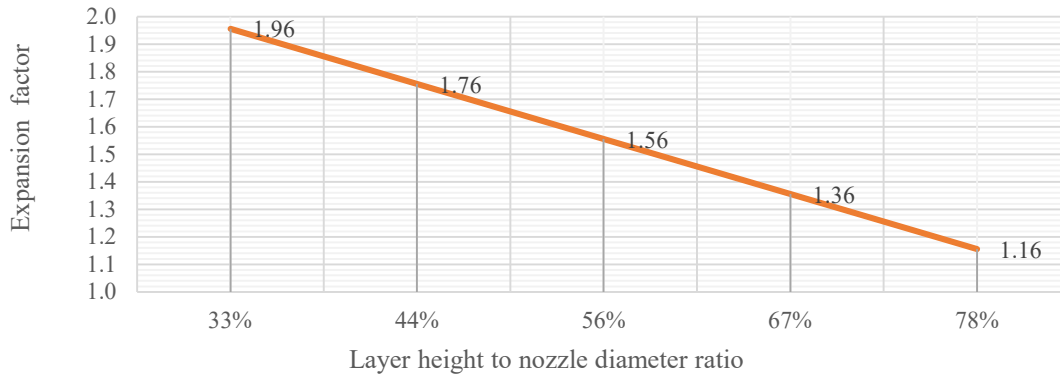
595

596 *Figure 19. Exploring the relationship between layer height and nozzle size*

Table 3. Description of the testing on the relationship between layer height, nozzle size and path line width.

Path line code	A	B	C	D	E	Unit
Scheme of path line cross section						--
Nozzle diameter (D)	45	45	45	45	45	mm

Layer height (h)	15	20	25	30	35	mm
Path width (w)	88	79	70	62	52	mm
Layer height to nozzle D ratio	33	44	56	67	78	%
Path width multiplication factor	1.96	1.76	1.56	1.36	1.16	--



597

598

Figure 20. Path line width estimation chart

599 The early estimation of path line's printed width has enabled the study team to implement a
600 code in the Grasshopper definition as part of the 3D model files to estimate the printed outcome
601 to provide informed decisions for geometry planning. For example, when planning to print a
602 cob wall that has a thickness of 500 mm, using a layer height of 25 mm would require a distance
603 of 430 mm between the two path lines creating the inner and outer sides of the wall. Increasing
604 the layer height to 30mm (while using the added definition in the 3D models) will then
605 automatically update the distance between the wall path lines to 448 mm.

606 In addition to the previous changes in path line width due the extrusion process and the forced
607 height by the nozzle, 3D printed cob encounters another cause of lateral deformation due to the
608 accumulative loads of each added layer. As the 3D printing process continues, more printed
609 layers accumulate on top of each other to create the desired height of the geometry. This
610 increase in loads leads to further slight lateral and longitudinal deformation as compared to the
611 original virtual model, where it is mostly seen in the bottom layers (Figure 21, left & right). It
612 was observed during all experiments that the level of deformation depends primarily on the
613 water content in the cob mix, as lower water content minimises the deformation to a negligible
614 level (Figure 21- left), which was an early prototype with 22% water content. The higher water
615 content of 24-25% leads to a noticeable deformation as in Figure 21- the prototype to the right,
616 where the gradual increase in layer heights is slightly noticeable from the bottom to the top
617 layers. Further exploration for the deformation aspects will be tested and presented in future
618 work.



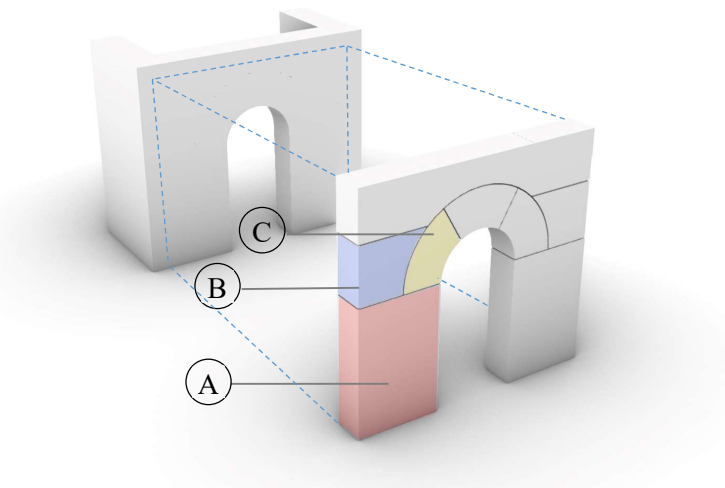
619

620 *Figure 21. Prototypes showing the longitudinal deformation due to accumulative weight of layers*
 621 *(lower water content to left, higher water content to the right).*

622 3.3. Geometry exploration

623 An exploration of various geometries was conducted to examine the capabilities of the 3D
 624 printing system. The study experimented with three types of geometries. The criteria of
 625 geometry selection were established on exploring the geometrical challenges that face the
 626 robotic 3D printing of a simple cob wall with an opening. Figure 22 suggests a traditional cob
 627 wall with arch-shaped opening to represent possible challenges while 3D printing cob walls,
 628 without using form work to create the openings. The challenges were found to be as follow:

- 629 A. Lift height (Max. height of continuous 3D printing)
- 630 B. Inclined 3-axis 3D printing (horizontal corbelling)
- 631 C. Inclined 6-axis 3D printing (radial corbelling)



632

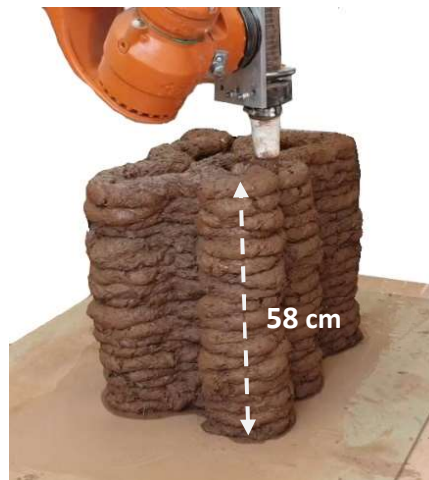
633 *Figure 22. Geometry challenges in a regular cob wall with an opening. 1) Lift height- 3 axis 3D*
 634 *printing; 2) Inclined 3-axis printing (corbelling); 3) Inclined 6-axis 3D printing.*

635 3.3.1. Lift height.

636 Cob walls are conventionally built of successive monolithic layers of earth called lifts. Each
 637 lift must be dry enough to a degree that enables it to bear the loads from the subsequent lifts.
 638 Lift height has an average of 60 cm. (Hamard et al. 2016; Weismann and Bryce 2006; Snell

639 and Callahan 2005). Hence, the first geometry exploration aimed to examine the maximum
640 height per lift (Figure 23). The geometry footprint was designed to have a rectangular footprint
641 of 60x40 cm, with a serpentine printing path line that creates the inner pattern of the wall. A
642 serpentine path line was selected for two reasons; first is to improve the structural performance
643 of the wall (Emmitt and Gorse 2005); second is to extend the printing time per each path line
644 as this should give more time for each layer to start drying and gain rigidity before receiving
645 the successive layers.

646 This test showed that the maximum stable height of the lift was 58 cm, very similar to the
647 traditional cob method. Exceeding this height increasingly jeopardised the stability of the
648 geometry and it starts showing toppling signs. This finding is also supported by the prototypes
649 by WASP (3D WASP 2016). This finding highlighted the importance of pausing or reducing
650 the 3D printing speed to give a chance to the freshly printed layers to settle properly and gain
651 more structural strength throughout the drying process.



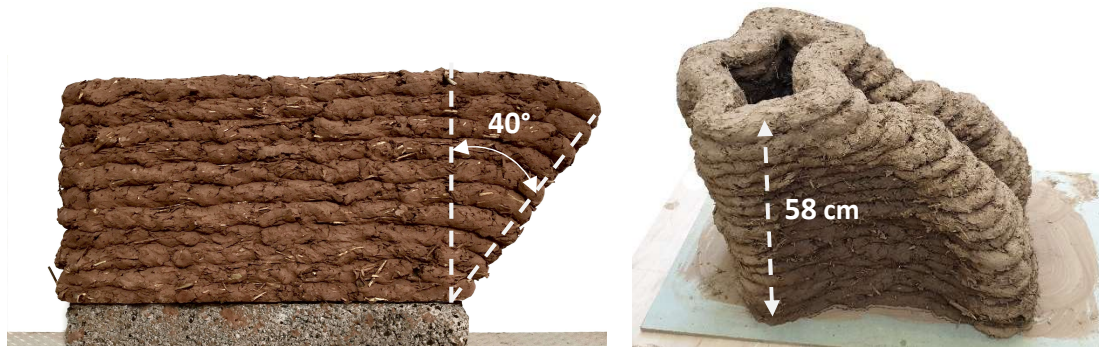
652

653 *Figure 23. Testing the maximum height per printing period.*

654 3.3.2. Inclined 3-axis 3D printing (horizontal corbelling)

655 The Second geometry exploration aimed to examine inclined 3-axis 3D printing, where the
656 corbelling happens in the horizontal XY plane only. The study examined two main approaches,
657 straight and gradual inclination (Figure 24, left-right). Based on several trials, it was found that
658 cob can sustain up to 40 degrees of straight inclination with 1:1.25 slope as shown in Figure
659 24-left. This was possible to achieve without using inner patterns but with slow printing speed
660 of 30 mm/sec. Based on several trials, it was observed that high inclinations (more than 40
661 degrees) are less stable and require denser design for inner patterns. On the other hand, using
662 gradual inclination required the addition of inner patterns to the geometry, but it showed a
663 possibility to achieve nearly 90 degrees of inclination as shown in Figure 24- left. However,
664 the increase of the inner pattern, in addition to the serpentine path line, caused a dramatic
665 consumption of material per unit volume.

666



667

668

669 *Figure 24. Examining the inclined 3-axis 3D printing; straight inclination (left) and gradual*
 670 *inclination (right)*

671 3.3.3. Inclined 6-axis 3D printing (radial corbelling)

672 The third exploration aimed to exercise a more complex style of movement that involved all
 673 the six axes of the robotic arm. Such added complexity can be leveraged to construct arch-
 674 based shapes, like catenary vaults and arches Figure 22-C. The test was able to achieve 45
 675 degrees of radial inclination in a one continuous print (Figure 25). It was possible to continue
 676 achieving higher degree of inclination, however, the geometry started to show instability due
 677 to its relatively small footprint (40 x 40 cm). It is worth mentioning that 75 degrees of
 678 inclination were successfully achieved in a previous study under this project using the small
 679 scale nozzle and less water content (Veliz Reyes et al. 2018). During the printing process of
 680 the arch prototype, the study observed that the 3D printed cob can gain structural strength from
 681 the ramming process, which is created by the extrusion forces and robotic arm compression.
 682 Also, similar to the previous two tests, it was necessary to add an inner pattern to geometry to
 683 increase the structural rigidity and the printing time per layer.

684



685

686 *Figure 25. Testing complex movement through 3D printing arch-based geometry.*

687 3.3.4. Remarks on geometry testing

688 Generally, the previous prototypes generated a record that has become useful to the planning
 689 of the future work on 3DP cob. Table 4 shows the different characteristics for each 3DP
 690 geometry. In addition, the testing process have revealed other factors which influence the
 691 geometry formation and its achieved quality. These factors are as follow:

- 692 • The overall footprint of the printed geometry: As longer foot prints, such as the external
693 walls of a small house for instance, means more time is spent in each layer, which
694 consequently enables the fresh 3D printed layers of cob to gain further strength as they
695 dry. The footprint of the geometries (e.g. Walls), can be also increased by designing
696 denser inner patterns inside the walls, which increase the stability of the printed
697 structure, and also improve the thermal performance (Gomaa et al. 2019).
- 698 • Layer height to path line ratio: As discussed earlier in section 3.2, lower layer height
699 creates wider path line. The increased footprint of path line offers greater stability to
700 the geometry. However, reducing the layer height means additional material is
701 consumed due to the increased number of required layers to reach the desired total
702 height of the geometry. This also will increase the overall printing time.
- 703 • The relation between printing velocity and hardening time: where this study did not test
704 systematically the competition between printing velocity and material hardening, the
705 study observed that shorter printing paths per layer jeopardise the ability of each printed
706 layer to harden sufficiently in order to sustain the loads of the successive layers. For
707 instance, in geometry 2, the small squared footprint created shorter printing path per
708 layer, which consequently required slower printing velocity, while in geometry 1, the
709 larger rectangular footprint enabled higher printing velocity. However, this issue can
710 be compensated by reducing the printing velocity or design the printing process to
711 follow longer paths. This explains why the extrusion rates as per Table 4 were all
712 maintained at 6.7 kg/ min while testing the current geometries despite the ability of
713 system to reach a flow rate of up to 11 kg/min. Worth mentioning that replacing the
714 empty cartridge manually takes nearly 30 seconds, which is less than the time needed
715 to extrude the other full cartridge This means that the extrusion does not stop at any
716 moment during the total printing process.

Table 4. The different characteristics for each 3DP geometry in the three tests.

	Test 1	Test 2	Test 3	Unit
Printing speed	50	50	50	mm/sec
Volume of printed cob	0.11	0.1	0.08	m ³
Weight of printed cob	198	182	132	kg
Number of used cartridges	16	15	11	
Total printing time	30	27	20	min
Extrusion rate	6.7	6.7	6.7	Kg/min

717 4. Conclusion

718 This paper presents a systematic study leveraging a traditional material and its associated
719 embodied knowledge as a driver for digital innovation, specifically to develop a low-cost and
720 sustainable alternative robotic 3D printing process and hardware (an extrusion system). The
721 construction industry has done substantial strides in the 3DP area since the development of
722 large-scale digital fabrication technologies (e.g. contour crafting). Several case studies and
723 prototypes greatly illustrate the potentials of these technologies beyond standard procurement
724 and standard building delivery models by integrating new knowledge into the building delivery

725 from areas such as manufacturing and robotics. In that context, this article advocates that
726 historical, traditional or vernacular material systems are a rich source of knowledge for further
727 research and innovation in the built environment sector, and provides a groundwork of material
728 resourcing, building knowledge and local skills with the potential for more sustainable
729 construction data-driven processes. The impact of this study can be outlined in three key areas:

- 730 1) The development of an innovative extrusion system for earth-based materials.
- 731 2) The development of a robotic 3DP system that provides the opportunity to prototype
732 new models of earth materials in the context of industrial frameworks of practice;
- 733 3) The leverage of vernacular material knowledge and skills to develop new technology
734 in the digital sector.

735 The system presented here involves material studies and printing characterisation parameters
736 as well as its associated hardware (an extrusion mechanism), and its implementation on small
737 scale tests. The development of this system involved building a series of prototypes through a
738 standard innovation delivery process, from basic ideation and research, up to proof of concept
739 and prototyping stages. Building upon standard liquid deposition modelling 3DP 3-axis
740 strategies, this system allows for more complex geometric configurations with more than 3
741 axis, and in contrast to traditional cob building processes, it allows for cob building elements
742 to be produced on the basis of a filament (forming a hollow geometry) instead of bulk mass-
743 based components, leading to higher geometrical flexibility, reduced material use and better
744 thermal efficiency as a result of air cavities.

745 This paper also contributes to architectural design research, as it acknowledges the material
746 cultural context as a springboard for digital and technological innovation delivery. This multi-
747 disciplinary approach reflects on the applicability of this technology in professional practice.
748 This project poses the concept of “material negotiation” to enable more flexible, open ended
749 and multi-disciplinary relationships between design and fabrication by using a recyclable and
750 reusable material prone to on-site modifications and adaptation. For instance, the dual extrusion
751 system allows for a decentralised production model by pre-packaging and procuring cob
752 cartridges from local suppliers and materials, reducing even further the construction’s carbon
753 footprint and involving knowledgeable local suppliers in the delivery plan.

754 The research suggests, however, further work to develop this system into an industrial demo
755 (and, even further, into a commercially viable system). Broadly, the research sets out a more
756 ambitious agenda addressing the need to acknowledge and further investigate the potential of
757 vernacular knowledge and buildings to facilitate material and digital manufacturing studies.
758 For instance, further work can explore the applicability of machine learning, material feedback
759 and computer vision approach for the robotic fabrication of building elements, as well as the
760 observation of craft and making practices as a way to develop more intelligent and responsive
761 manufacturing systems. Specifically to this study, the extrusion system would benefit from a
762 higher degree of automation by developing a feeding system where cartridges are loaded and
763 unloaded into the extrusion mechanism, ready to deliver material for 3D printing and where
764 empty tubes can be collected and re-filled. A simple computation of printing speed, volume,
765 and daily schedule can inform the size of buffer needed for pre-filled tubes and the required
766 rate of exchange and delivery, which will greatly improve the degree of automation of the
767 system enabling larger continuous prints. Also, in terms of local markets and the need to
768 refurbish and repair existing cob structures, we envisage this technology as a useful alternative

769 for cob building maintenance (e.g. crack filling, construction of pre-dried cob blocks), in
770 alignment with recent strides on the use of robotic technology and intelligent computer vision
771 for building maintenance applications, such as autonomous crack detection.

772 **5. Acknowledgements**

773 We would like to acknowledge Jack Francis and Dr Peter Theobald for their valuable
774 collaboration and support (Cardiff University). We also extend our gratitude to Aikaterini
775 Chatzivasileiadi and Anas Lila (Cardiff University) for their invaluable help. Special thanks
776 also must be made to EMAR Engineering Services in Egypt for their technical support.

777 **6. Funding sources**

778 This work was supported financially by the Engineering and Physical Sciences Research
779 Council (EPSRC) and The University of Nottingham under the Network Plus: Industrial
780 Systems in the Digital Age, Grant number: EP/P001246/1.

781 This work is also partially supported financially by the University of Adelaide through the
782 Research Abroad Scholarship scheme.

783 **7. References**

- 784 3D-WASP. 2020. “3D Printers | WASP | Leading Company in the 3d Printing Industry.”
785 2020. <https://www.3dwasp.com/en/>. [accessed 31-08-2020]
- 786 3D WASP. 2016. “The Clay and Straw Wall by The 3 M| Stampanti 3D | WASP.” 2016.
787 <https://www.3dwasp.com/en/il-muro-di-terra-e-paglia-alle-soglie-dei-3-metri/>. [accessed
788 31-08-2020]
- 789 Agustí-Juan, Isolda, Florian Müller, Norman Hack, Timothy Wangler, and Guillaume Habert.
790 2017. “Potential Benefits of Digital Fabrication for Complex Structures: Environmental
791 Assessment of a Robotically Fabricated Concrete Wall.” *Journal of Cleaner Production* 154:
792 pp 330–340. <https://doi.org/10.1016/j.jclepro.2017.04.002>.
- 793 Alhumayani, Hashem, Mohamed Gomaa, Veronica Soebarto, and Wassim Jabi. 2020.
794 “Environmental Assessment of Large-Scale 3D Printing in Construction: A Comparative
795 Study between Cob and Concrete.” *Journal of Cleaner Production* 270 (June): pp 122463-
796 122488. <https://doi.org/10.1016/j.jclepro.2020.122463>.
- 797 Benardos, A., I. Athanasiadis, and N. Katsoulakos. 2014. “Modern Earth Sheltered
798 Constructions: A Paradigm of Green Engineering.” *Tunnelling and Underground Space*
799 *Technology* 41 (1): pp 46–52. <https://doi.org/10.1016/j.tust.2013.11.008>.
- 800 Bruno, Agostino Walter, Domenico Gallipoli, Céline Perlot, and Joao Mendes. 2017.
801 “Mechanical Behaviour of Hypercompacted Earth for Building Construction.” *Materials*
802 *and Structures/Materiaux et Constructions* 50 (2): pp 160-175.
803 <https://doi.org/10.1617/s11527-017-1027-5>.
- 804 Choi, Myoung Sung, Young Jin Kim, and Jin Keun Kim. 2014. “Prediction of Concrete
805 Pumping Using Various Rheological Models.” *International Journal of Concrete Structures*
806 *and Materials* 8 (4): pp 269–278. <https://doi.org/10.1007/s40069-014-0084-1>.
- 807 ContourCrafting. 2020. “Building Construction - CC-Corp.” 2020.
808 <https://contourcrafting.com/building-construction/>. [accessed 08-02-2020]
- 809 Emmitt, Stephen, and Christopher A. Gorse. 2005. *Barry’s Introduction to Construction of*
810 *Buildings*. Cornwall: Blackwell Publishing Ltd. ISBN 1-4051-1055-4.

811 Garrett, Banning. 2014. "3D Printing: New Economic Paradigms and Strategic Shifts."
812 *Global Policy* 5 (1): pp 70–75. <https://doi.org/10.1111/1758-5899.12119>.

813 Geneidy, Omar, Walaa S.E. Ismaeel, and Ayman Abbas. 2019. "A Critical Review for
814 Applying Three-Dimensional Concrete Wall Printing Technology in Egypt." *Architectural*
815 *Science Review* 0 (0): pp 1–15. <https://doi.org/10.1080/00038628.2019.1596066>.

816 Gomaa, Mohamed, Jim Carfrae, Steve Goodhew, Wassim Jabi, and Alejandro Veliz Reyez.
817 2019. "Thermal Performance Exploration of 3D Printed Cob." *Architectural Science*
818 *Review*, April, pp 1–8. <https://doi.org/10.1080/00038628.2019.1606776>.

819 Goodhew, Steve, P.C. Grindley, and S.D. Probeif. 1995. "Composition, Effective Thermal
820 Conductivity And Specific Heat Of Cob Earth-Walling." *WIT Transactions on The Built*
821 *Environment* 15 (1): pp 205-217. <https://doi.org/10.2495/STR950231>.

822 Goodhew, Steven, and Richard Griffiths. 2005. "Sustainable Earth Walls to Meet the
823 Building Regulations." *Energy and Buildings* 37 (2005): pp 451-459. Elsevier.
824 <https://doi.org/10.1016/j.enbuild.2004.08.005>.

825 Hamard, Erwan, Bogdan Cazacliu, Andry Razakamanantsoa, and Jean Claude Morel. 2016.
826 "Cob, a Vernacular Earth Construction Process in the Context of Modern Sustainable
827 Building." *Building and Environment* 106 (1): pp 103–119.
828 <https://doi.org/10.1016/j.buildenv.2016.06.009>.

829 Kennedy, Joseph F., Michael G. Smith, and Catherine Wanek. 2015. *The Art of Natural*
830 *Building*. Edited by C Wanek, M Smith, and JF Kennedy. Vancouver, Canada: New Society
831 Publishers. ISBN: 0865714339

832 Khan Academy. 2015. "What Is Volume Flow Rate? (Article) | Fluids | Khan Academy."
833 2015. [https://www.khanacademy.org/science/physics/fluids/fluid-dynamics/a/what-is-](https://www.khanacademy.org/science/physics/fluids/fluid-dynamics/a/what-is-volume-flow-rate)
834 [volume-flow-rate](https://www.khanacademy.org/science/physics/fluids/fluid-dynamics/a/what-is-volume-flow-rate). [accessed 01-09-2020]

835 Khelifi, H., A. Perrot, T. Lecompte, and G. Ausias. 2013. "Design of Clay/Cement Mixtures
836 for Extruded Building Products." *Materials and Structures/Materiaux et Constructions* 46
837 (6): pp 999–1010. <https://doi.org/10.1617/s11527-012-9949-4>.

838 Kothman, Ivo, and Niels Faber. 2016. "How 3D Printing Technology Changes the Rules of
839 the Game Insights from the Construction Sector." *Journal of Manufacturing Technology*
840 *Management* 27 (7): pp 932–943. <https://doi.org/10.1108/JMTM-01-2016-0010>.

841 Le, H. D., E. H. Kadri, S. Aggoun, J. Vierendeels, P. Troch, and G. De Schutter. 2015.
842 "Effect of Lubrication Layer on Velocity Profile of Concrete in a Pumping Pipe." *Materials*
843 *and Structures/Materiaux et Constructions* 48 (12): pp 3991–4003.
844 <https://doi.org/10.1617/s11527-014-0458-5>.

845 Le, T. T., S. A. Austin, S. Lim, R. A. Buswell, R. Law, A. G.F. Gibb, and T. Thorpe. 2012.
846 "Hardened Properties of High-Performance Printing Concrete." *Cement and Concrete*
847 *Research* 42 (3): pp 558–666. <https://doi.org/10.1016/j.cemconres.2011.12.003>.

848 Leu, Ming C., Lie Tang, Brad Deuser, Robert G. Landers, Gregory E. Hilmas, Shi Zhang,
849 and Jeremy Watts. 2011. "Freeze-Form Extrusion Fabrication of Composite Structures."
850 *22nd Annual International Solid Freeform Fabrication Symposium - An Additive*
851 *Manufacturing Conference, (2011: Aug. 8-10, Austin, TX)* pp 111–124. University of Texas
852 at Austin. <https://www.researchgate.net/publication/266522915>

853 Lipscomb, G. G., and M. M. Denn. 1984. "Flow of Bingham Fluids in Complex Geometries."
854 *Journal of Non-Newtonian Fluid Mechanics* 14 (C): pp 337–346.
855 [https://doi.org/10.1016/0377-0257\(84\)80052-X](https://doi.org/10.1016/0377-0257(84)80052-X).

856 Niroumand, Hamed, Juan Antonio Barceló Álvarez, and Maryam Saaly. 2016. "Investigation
857 of Earth Building and Earth Architecture According to Interest and Involvement Levels in
858 Various Countries." *Renewable and Sustainable Energy Reviews* 57: pp 1390–1397.
859 <https://doi.org/10.1016/j.rser.2015.12.183>.

860 Panda, Biranchi, and Ming Jen Tan. 2018. "Experimental Study on Mix Proportion and Fresh

861 Properties of Fly Ash Based Geopolymer for 3D Concrete Printing.” *Ceramics*
862 *International* 44 (9): pp 10258–10265. <https://doi.org/10.1016/j.ceramint.2018.03.031>.

863 Panda, Biranchi, Cise Unluer, and Ming Jen Tan. 2018. “Investigation of the Rheology and
864 Strength of Geopolymer Mixtures for Extrusion-Based 3D Printing.” *Cement and Concrete*
865 *Composites* 94 (November 2017): pp 307–314.
866 <https://doi.org/10.1016/j.cemconcomp.2018.10.002>.

867 Perrot, A., D. Rangeard, and E. Courteille. 2018. “3D Printing of Earth-Based Materials:
868 Processing Aspects.” *Construction and Building Materials* 172: pp 670–676.
869 <https://doi.org/10.1016/j.conbuildmat.2018.04.017>.

870 Perrot, A., D. Rangeard, and T. Lecompte. 2018. “Field-Oriented Tests to Evaluate the
871 Workability of Cob and Adobe.” *Materials and Structures/Materiaux et Constructions* 51
872 (2): pp 1–10. <https://doi.org/10.1617/s11527-018-1181-4>.

873 Perrot, A, D Rangeard, and A Pierre. 2016. “Structural Built-up of Cement-Based Materials
874 Used for 3D- Printing Extrusion Techniques.” *Materials and Structures/Materiaux et*
875 *Constructions* 49: pp 1213–1220. <https://doi.org/10.1617/s11527-015-0571-0>.

876 Shakor, Pshtiwan, Shami Nejadi, Gavin Paul, and Sardar Malek. 2019. “Review of Emerging
877 Additive Manufacturing Technologies in 3d Printing of Cementitious Materials in the
878 Construction Industry.” *Frontiers in Built Environment* 4: 85 pp 1-17.
879 <https://doi.org/10.3389/fbuil.2018.00085>.

880 Snell, Clarke., and Tim Callahan. 2005. *Building Green : A Complete How-to Guide to*
881 *Alternative Building Methods : Earth Plaster, Straw Bale, Cordwood, Cob, Living Roofs*.
882 Lark Books. ISBN: 9781579905323

883 Tay, Yi Wei Daniel, Biranchi Panda, Suvash Chandra Paul, Nisar Ahamed Noor Mohamed,
884 Ming Jen Tan, and Kah Fai Leong. 2017. “3D Printing Trends in Building and Construction
885 Industry: A Review.” *Virtual and Physical Prototyping* 12 (3): pp 261–276.
886 <https://doi.org/10.1080/17452759.2017.1326724>.

887 Veliz Reyes, Alejandro, Mohamed Gomaa, Aikaterini Chatzivasileiadi, and Wassim Jabi.
888 2018. “Computing Craft: Early Stage Development Ofa Robotically-Supported 3D Printing
889 System for Cob Structures.” *Proceedings of the 34th Conference of Education in Computer*
890 *Aided Architectural Design in Europe (eCAADe)- Computing for Better Tomorrow*, 1: pp
891 791–800. Lodz: cuminCad. <https://pearl.plymouth.ac.uk/handle/10026.1/12769>

892 Veliz Reyes, Alejandro, Wassim Jabi, Mohamed Gomaa, Aikaterini Chatzivasileiadi, Lina
893 Ahmad, and Nicholas Mario Wardhana. 2019. “Negotiated Matter: A Robotic Exploration
894 of Craft-Driven Innovation.” *Architectural Science Review* 0 (0): pp 1–11.
895 <https://doi.org/10.1080/00038628.2019.1651688>.

896 Weismann, Adam, and Katy Bryce. 2006. *Building with Cob: A Step-by-Step Guide*. Devon:
897 Green Books ltd. ISBN: 1903998727

898 Wu, Peng, Jun Wang, and Xiangyu Wang. 2016. “A Critical Review of the Use of 3-D
899 Printing in the Construction Industry.” *Automation in Construction* 68: pp 21–31.
900 <https://doi.org/10.1016/j.autcon.2016.04.005>.

901 Zareiyan, Babak, and Behrokh Khoshnevis. 2017. “Interlayer Adhesion and Strength of
902 Structures in Contour Crafting - Effects of Aggregate Size, Extrusion Rate, and Layer
903 Thickness.” *Automation in Construction* 81 (June): pp 112–121.
904 <https://doi.org/10.1016/j.autcon.2017.06.013>.

905 Zhang, Xu, Mingyang Li, Jian Hui Lim, Yiwei Weng, Yi Wei Daniel Tay, Hung Pham, and
906 Quang Cuong Pham. 2018. “Large-Scale 3D Printing by a Team of Mobile Robots.”
907 *Automation in Construction* 95 (August): pp 98–106.
908 <https://doi.org/10.1016/j.autcon.2018.08.004>
909